UC Merced
UC Merced Previously Published Works

Title

One-way radiative transfer

Permalink

https://escholarship.org/uc/item/9c02t8bt

Authors

González-Rodríguez, Pedro
Ilan, Boaz
Kim, Arnold D

Publication Date

2016-06-01

DOI

10.1016/j.jqsrt.2016.02.032

Peer reviewed

One-way radiative transfer

Pedro González-Rodríguez [a], Boaz Ilan [b], Arnold D. Kim [b,*]

[a] Gregorio Millán Institute, Universidad Carlos III de Madrid, Leganés 28911, Spain
[b] Applied Mathematics Unit, School of Natural Sciences, University of California, Merced, 5200 North Lake Road, Merced, CA 95343, USA

A B S T R A C T

We introduce the one-way radiative transfer equation (RTE) for modeling the transmission of a light beam incident normally on a slab composed of a uniform forward-peaked scattering medium. Unlike the RTE, which is formulated as a boundary value problem, the one-way RTE is formulated as an initial value problem. Consequently, the one-way RTE is much easier to solve. We discuss the relation of the one-way RTE to the Fokker–Planck, small-angle, and Fermi pencil beam approximations. Then, we validate the one-way RTE through systematic comparisons with RTE simulations for both the Henyey–Greenstein and screened Rutherford scattering phase functions over a broad range of albedo, anisotropy factor, optical thickness, and refractive index values. We find that the one-way RTE gives very good approximations for a broad range of optical property values for thin to moderately thick media that have moderately to sharply forward-peaked scattering. Specifically, we show that the error made by the one-way RTE decreases monotonically as the anisotropic factor increases and as the albedo increases. On the other hand, the error increases monotonically as the optical thickness increases and the refractive index mismatch at the boundary increases.

© 2016 Elsevier Ltd. All rights reserved.

1. Introduction

Radiative transfer theory governs the propagation of light in a multiple scattering (turbid) medium [1,2]. One particularly important problem in radiative transfer is determining the transmission of a collimated beam incident normally on a plane-parallel slab. This problem has important applications in atmospheric and ocean optics [3,4], and biomedical optics [5], among others. In all of these applications, one seeks to determine optical properties of the medium from spatially-resolved transmission measurements. This problem remains a challenge because the governing boundary value problem for the radiative transfer equation (RTE) is difficult to solve. For this reason,

developing accurate approximations that are easier to solve is useful.

A prominent feature that clouds, oceans and biological tissues often exhibit is forward-peaked scattering, *i.e.*, most of the power scattered by the medium flows in the same direction as it is incident. Forward-peaked scattering is challenging computationally because it requires extensive resources to adequately resolve the sharp peak in the scattering phase function. Therefore, a number of useful approximations have been derived to deal with this scenario. In particular, the asymptotic limit of sharply forward-peaked scattering has been studied extensively leading to the Fokker–Planck approximation [6,7] and its generalizations [8–11]. However, these approximations all lead to the same kind of *boundary value problem* as for the RTE. In this respect, the Fokker–Planck type approximations are also relatively complicated to solve. Moreover, these approximations are derived for the extreme case of a

very sharply peaked forward scattering. Therefore, rather than being broadly applicable, the accuracy of these models tends to be case-dependent.

An alternative approach is to approximate the RTE with an *initial value problem*, which is much easier to solve. In particular, the small-angle approximation [2] has been studied extensively with recent applications to polarized media [12] and atmospheric optics [13]. In the small-angle approximation, the transport operator in the RTE is simplified with a purely advective operator in the forward direction. A further reduction of the small-angle approximation leads to the Fermi pencil-beam approximation [14–17], which can be solved analytically. However, as the beam penetrates deeply into a turbid medium, it spreads in both space and angle beyond the region of validity of these approximations. Consequently, the small-angle and Fermi pencil-beam approximations become inaccurate in optically thick media.

Here, we introduce the one-way RTE, which is derived by restricting the limits of integration in the scattering operator to the hemisphere of directions aligned with the incident direction of the collimated beam. This truncation is tantamount to neglecting multiple backscattering in the problem. This approach has been used extensively in wave equation migration problems in geophysics [18,19], for example, from which we inherit the "one-way" terminology. The result from this approximation is an initial-value problem that is easier to solve, allows for forward peaked scattering that need not be sharp, and retains dependence between the angular and spatial nature of the radiation in the forward hemisphere. In this way, the one-way RTE addresses the limitations of the aforementioned approximations. In fact, this approximation has been recently applied to study diffuse optical tomography in biological tissues [20] and shown to be useful. Additionally, the one-way RTE has been derived rigorously using the theory of waves in random media [21].

The outline of the paper is as follows. Section 2 describes the boundary value problem for the (full) RTE that governs a beam incident normally on a slab, which is composed of a uniform scattering and absorbing medium. We consider here the general case in which the refractive index within the slab is different from that outside of the slab. In Section 3 we introduce the one-way RTE and the associated initial value problem for beam transmission through the slab. Section 4 contains numerical results that compare simulations using the full RTE with solutions of one-way RTE over a broad range of optical parameters. Section 5 contains the conclusions and discussion of the results.

2. The radiative transfer equation

Let I denote the intensity that depends on direction, $\hat{\mathbf{s}}$, which is a vector on the unit sphere, $\mathbb{S}^2$, and position $\mathbf{r}$. In a multiple scattering medium, I is governed by the RTE,

$$\hat{\mathbf{s}} \cdot \nabla I + I = \varpi_0 \int_{\mathbb{S}^2} p(\hat{\mathbf{s}} \cdot \hat{\mathbf{s}}') I(\hat{\mathbf{s}}', \mathbf{r}) \, \mathrm{d}\hat{\mathbf{s}}', \tag{2.1}$$

where ϖ_0 is the single scattering albedo. In (2.1) we have used the standard non-dimensional spatial variables,

which are rescaled according to $\mathbf{r} = (\mu_a + \mu_s)\tilde{\mathbf{r}}$, with μ_a and μ_s denoting the absorption coefficient. The scattering phase function, $p(\hat{\mathbf{s}} \cdot \hat{\mathbf{s}}')$, gives the fraction of light scattered in direction $\hat{\mathbf{s}}$ due to light incident in direction $\hat{\mathbf{s}}'$. Here, we consider two different scattering phase functions: the Henyey–Greenstein and screened Rutherford scattering phase functions. The Henyey–Greenstein scattering phase function is defined as

$$p(\hat{\mathbf{s}} \cdot \hat{\mathbf{s}}') = \frac{1}{4\pi} \frac{1 - g^2}{(1 + g^2 - 2g\hat{\mathbf{s}} \cdot \hat{\mathbf{s}}')^{3/2}}, \tag{2.2}$$

with g denoting the anisotropy factor. For different media, the value of g can range between 0 and 1. In particular, $g = 0$ corresponds to an isotropic scattering medium, whereas the limit $g \to 1$ corresponds to scattering only in the forward direction. This scattering phase function is particularly useful since it allows one to continuously vary a single parameter, g, which controls the sharpness of forward-peaked scattering. The screened Rutherford phase function is defined as

$$p(\hat{\mathbf{s}} \cdot \hat{\mathbf{s}}') = \frac{2\eta(\eta + 1)}{(1 + 2\eta - \hat{\mathbf{s}} \cdot \hat{\mathbf{s}}')^2}, \tag{2.3}$$

where $\eta > 0$ is a typically small constant called the screening parameter. As $\eta \to 0$, (2.3) becomes more forward-peaked. Both of these scattering phase functions are normalized according to

$$\int_{\mathbb{S}^2} p(\hat{\mathbf{s}} \cdot \hat{\mathbf{s}}') \mathrm{d}\hat{\mathbf{s}}' = 1. \tag{2.4}$$

We are interested in studying the transmission of a Gaussian beam incident normally on the three-dimensional slab, $\{(x, y, z) | -\infty < x, y < \infty, 0 < z < z_0\}$, composed of a uniform absorbing and scattering medium. The refractive index inside the slab can be different from medium on either side of the slab. For that reason, we must take into account partial reflections at the boundaries due to this refractive index mismatch. For this problem we seek the solution of (2.1) in $0 < z < z_0$ subject to the boundary conditions that we specify below.

The collimated beam is incident on the boundary, $z = 0$, and the associated boundary condition is

$$I(\hat{\mathbf{s}}, x, y, 0) = t_1(\hat{z})\delta(\hat{\mathbf{s}} - \hat{z})b(x, y) + r_1(\hat{\mathbf{s}}_1 \to \hat{\mathbf{s}})I(\hat{\mathbf{s}}_1, x, y, 0) \quad \text{on}$$
$$\hat{\mathbf{s}} \cdot \hat{z} > 0, \tag{2.5}$$

where $\delta(\cdot)$ is the Dirac delta function, and

$$b(x, y) = \frac{2P_0}{\pi R^2} \exp\left[-2(x^2 + y^2)/R^2\right]. \tag{2.6}$$

The first term in boundary condition (2.5) corresponds to the Gaussian beam defined in (2.6) incident normally on and transmitted across the boundary $z = 0$. Here, $t_1(\hat{z})$ denotes the Fresnel transmission coefficient for light incident on the boundary from outside of the slab in direction $\hat{z}$. The total power of the beam is denoted by P_0, and the $1/e^2$ radius of the beam is denoted by R. The second term in boundary condition (2.5) corresponds to the reflection of light incident on the $z = 0$ boundary from within the slab in direction $\hat{\mathbf{s}}_1$ with $\hat{\mathbf{s}}_1 \cdot \hat{z} < 0$ and reflected in direction $\hat{\mathbf{s}}$ as governed by Snell's law. Here, $r_1(\hat{\mathbf{s}}_1 \to \hat{\mathbf{s}})$ denotes the

Fresnel reflection coefficient for light incident on the boundary from within the slab.

There is no incident radiation on the boundary, $z = z_0$, from outside of the slab. Thus, the boundary condition on $z = z_0$ is

$$I(\hat{s}, x, y, z_0) = r_2(\hat{s}_2 \to \hat{s})I(\hat{s}_2, x, y, z_0) \quad \text{on } \hat{s} \cdot \hat{z} < 0. \quad (2.7)$$

Here, $r_2(\hat{s}_2 \to \hat{s})$ denotes the Fresnel reflection coefficient for light incident on the $z = z_0$ boundary from within the slab in direction $\hat{s}_2$ with $\hat{s}_2 \cdot \hat{z} > 0$ as governed by Snell's law.

Upon solution of the boundary value problem consisting of (2.1) subject to boundary conditions (2.5) and (2.7), we obtain $I(\hat{s}, x, y, z)$. To study the transmission of this beam, we compute the transmittance, defined as

$$T(x, y) = \int_{\hat{s} \cdot \hat{z} > 0} t_2(\hat{s}' \to \hat{s})I(\hat{s}', x, y, z_0)\hat{s} \cdot \hat{z} \, d\hat{s}. \quad (2.8)$$

Here, $t_2(\hat{s}' \to \hat{s})$ is the Fresnel transmission coefficient for light incident on the $z = z_0$ boundary from within the slab in direction $\hat{s}'$ with $\hat{s}' \cdot \hat{z} > 0$ transmitted in direction $\hat{s}$ as governed by Snell's law. In the results that follow, we compute the diffuse transmittance, T_d, which is defined by (2.8) with I replaced by the diffuse intensity I_d.

3. The one-way radiative transfer equation

Let $\mu = \cos \theta$ denote the cosine of the polar angle and φ denote the azimuthal angle. Then (2.1) can be written in terms of μ and φ as

$$\mu \partial_z I + \sqrt{1-\mu^2}(\cos \varphi \partial_x I + \sin \varphi \partial_y I) + I$$
$$= \varpi_0 \int_0^{2\pi} \int_{-1}^{1} p(\mu, \mu', \varphi - \varphi')I(\mu', \varphi', x, y, z) \, d\mu' \, d\varphi'. \quad (3.1)$$

Boundary condition (2.4) becomes

$$I(\mu, \varphi, x, y, 0) = t_1(\hat{z})\frac{\delta(\mu-1)}{2\pi}b(x, y) + r_1(\mu)I(-\mu, \varphi, x, y, 0) \quad \text{on}$$
$$0 < \mu \leq 1. \quad (3.2)$$

Boundary condition (2.6) becomes

$$I(\mu, \varphi, x, y, z_0) = r_2(\mu)I(-\mu, \varphi, x, y, z_0) \quad \text{on } -1 \leq \mu < 0. \quad (3.3)$$

Note that we have incorporated Snell's law explicitly in boundary conditions (3.2) and (3.3).

3.1. Deriving the one-way RTE

We now introduce the forward and backward half-range intensities, defined as

$$I^{\pm} = I(\pm\mu, \varphi, x, y, z) \quad \text{for } 0 < \mu \leq 1, \quad (3.4)$$

respectively. It follows from (3.1) that $I^{\pm}$ satisfy two coupled RTEs,

$$\pm \mu \partial_z I^{\pm} + \sqrt{1-\mu^2}(\cos \varphi \partial_x I^{\pm} + \sin \varphi \partial_y I^{\pm}) + I^{\pm}$$
$$= \varpi_0 \mathcal{P}_f I^{\pm} + \varpi_0 \mathcal{P}_b I^{\mp}. \quad (3.5)$$

Here, we have defined the forward and backward scattering operators,

$$\mathcal{P}_{f,b} = \int_0^{2\pi} \int_0^1 p_{f,b}(\mu, \mu', \varphi - \varphi')[\cdot] \, d\mu' \, d\varphi' \quad (3.6)$$

with p_f and p_b denoting the forward and backward scattering phase functions, respectively, which are restrictions of the original scattering phase function, i.e., $p_f = p(\mu, \mu', \varphi - \varphi') = p(-\mu, -\mu', \varphi - \varphi')$ and $p_b = p(\mu, -\mu', \varphi - \varphi') = p(-\mu, \mu', \varphi - \varphi')$ for $0 < \mu, \mu' \leq 1$. Note that the two equations in (3.5) are coupled because $I^{\mp}$ appears on the right-hand side. In terms of $I^{\pm}$, boundary condition (3.2) is given as

$$I^+(\mu, \varphi, x, y, 0) = t_1(\hat{z})\frac{\delta(\mu-1)}{2\pi}b(x, y) + r_1(\mu)I^-(\mu, \varphi, x, y, 0), \quad (3.7)$$

and boundary condition (3.3) is given as

$$I^-(\mu, \varphi, x, y, z_0) = r_2(\mu)I^+(\mu, \varphi, x, y, z_0). \quad (3.8)$$

Both boundary conditions (3.7) and (3.8) are on $0 < \mu \leq 1$. It is important to note that no approximations of the problem have been introduced thus far. In fact, the boundary value problem comprised of (3.5) subject to boundary conditions (3.7) and (3.8) is equivalent to the boundary value problem for the RTE given above.

Now we consider anisotropic scattering which is forward peaked. Because of the normalization given in (2.3), the "mass" contained in the forward hemisphere, $\hat{s} \cdot \hat{z} > 0$, is defined as

$$M_f = \int_{\hat{s}' \cdot \hat{z} > 0} p(\hat{z} \cdot \hat{s}') \, d\hat{s}' = 2\pi \int_0^1 p(\xi) \, d\xi. \quad (3.9)$$

For isotropic scattering, i.e., when $g = 0$, $M_f = 1/2$. For purely forward scattering, i.e., when $g \to 1$, $M_f \to 1$. Fig. 1 is a plot of M_f for the Henyey–Greenstein scattering phase function (2.2) for $0 \leq g \leq 1$, and for the screened Rutherford scattering phase function (2.3) for values of η that yield an effective anisotropy factor, g_{eff}, to be $0 \leq g_{\text{eff}} \leq 1$.

For $g > 0.65$, we find that M_f contains over 90% of the total mass for both scattering phase functions. Therefore, for these values of g it follows that $\|\mathcal{P}_f I^{\pm}\| \gg \|\mathcal{P}_b I^{\mp}\|$. In light of this observation, we neglect the $\mathcal{P}_b I^-$ term in (3.5), and find that I^+ satisfies the approximate equation,

$$\mu \partial_z I^+ + \sqrt{1-\mu^2}(\cos \varphi \partial_x I^+ + \sin \varphi \partial_y I^+) + I^+ = \varpi_0 \mathcal{P}_f I^+. \quad (3.10)$$

We call (3.10) the one-way RTE, because it describes the (approximate) behavior of I^+. Notice that I^- does not appear at all in (3.10) for a collimated beam transmitting through a forward-peaked medium. Similarly, by neglecting the second term in boundary condition (3.7), we obtain the "initial" condition,

$$I^+(\mu, \varphi, x, y, 0) = t_1(\hat{z})\frac{\delta(\mu-1)}{2\pi}b(x, y) \quad \text{on } 0 < \mu \leq 1. \quad (3.11)$$

Eq. (3.10) together with the initial condition (3.11) comprise an initial value problem for the forward intensity. Upon solution of this initial value problem, we compute
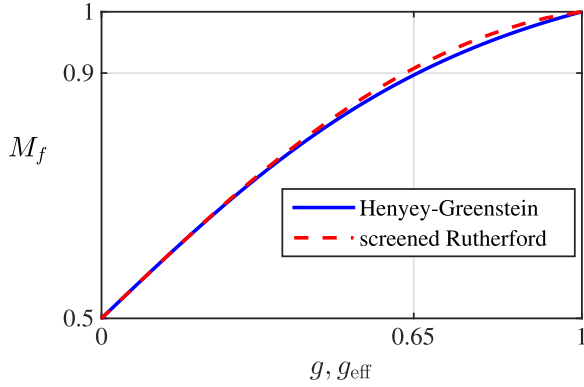
Fig. 1. The mass contained in the forward hemisphere of the Henyey–Greenstein (2.2), and the screened Rutherford scattering phase functions (2.3) [see (3.9)].

the transmittance through the slab through evaluation of

$$T(x,y) = \int_0^{2\pi} \int_0^1 t_2(\mu' \to \mu) I^+(\mu', \varphi, x, y, z_0) \mu \, d\mu \, d\varphi. \quad (3.12)$$

3.2. The one-way RTE as a first-iteration of the RTE

It is interesting to point out that the initial value problem comprised of (3.10) subject to initial condition (3.11) is the first iteration of the following iteration scheme for solving the coupled system (3.5).

1. Set $I^{(0)-} = 0$ (corresponding to $n=0$) and $n=1$.
2. Solve the initial value problem for the forward propagating radiance

$$\mu \partial_z I^{(n)+} + \sqrt{1-\mu^2}(\cos \varphi \partial_x I^{(n)+} + \sin \varphi \partial_y I^{(n)+}) + I^{(n)+}$$
$$- \varpi_0 \mathcal{P}_f I^{(n)+} = \varpi_0 \mathcal{P}_b I^{(n-1)-},$$

in $0 < z \leq z_0$ subject to

$$I^{(n)+}(\mu, \varphi, x, y, 0) = t_1(\hat{z}) \frac{\delta(\mu-1)}{2\pi} b(x,y)$$
$$+ r_1(\mu) I^{(n-1)-}(\mu, \varphi, x, y, 0).$$

3. Solve the final value problem for the backward propagating radiance

$$-\mu \partial_z I^{(n)-} + \sqrt{1-\mu^2}(\cos \varphi \partial_x I^{(n)-} + \sin \varphi \partial_y I^{(n)-}) + I^{(n)-}$$
$$- \varpi_0 \mathcal{P}_f I^{(n)-} = \varpi_0 \mathcal{P}_b I^{(n)+}$$

in $z_0 > z \geq 0$ subject to

$$I^{(n)-}(\mu, \varphi, x, y, z_0) = r_2(\mu) I^{(n)+}(\mu, \varphi, x, y, z_0).$$

4. Repeat Steps 2 through 4 for $n \leftarrow n+1$ until convergence is reached.

The complete solution of the original RTE problem is given by (3.4).

In contrast to the conventional source iteration method [22], which computes the scattering integral over all directions, this iteration scheme is the same as the improved source-iteration introduced by Gao and Zhao [23].

3.3. Numerical method

We focus our attention on computation of the diffuse forward intensity, I_d^+, which satisfies

$$\mu \partial_z I_d^+ + \sqrt{1-\mu^2}(\cos \varphi \partial_x I_d^+ + \sin \varphi \partial_y I_d^+) + I_d^+$$
$$= \varpi_0 \mathcal{P}_f I_d^+ + Q_{ri}^+, \quad (3.13)$$

with

$$Q_{ri}^+ = \mathcal{P}_f I_{ri}^+ = t_1(\hat{z}) \varpi_0 p_f(\mu, 1, \cdot) b(x,y) e^{-z}, \quad (3.14)$$

subject to initial condition

$$I_d(\mu, \varphi, x, y, 0) = 0 \quad \text{on } 0 < \mu \leq 1. \quad (3.15)$$

Upon solution of the initial value problem for I_d^+ comprised of (3.13) subject to initial condition (3.15), we then compute the one-way RTE approximation of the diffuse transmittance through evaluation of

$$T_d(x,y) = \int_0^{2\pi} \int_0^1 t_2(\mu' \to \mu) I_d^+(\mu', \varphi, x, y, z_0) \mu \, d\mu \, d\varphi. \quad (3.16)$$

The one-way RTE offers high potential for efficiency gains since numerical methods for initial value problems are generally simpler and more efficient than those for boundary value problems. For example, no iterations such as those described in Section 3.2 are needed to solve the one-way RTE. All that is required is a "time-stepping" method that advances the solution from $z=0$ to $z=z_0$. One such method is used in [20]. In contrast, solving the full RTE requires several iterations which depends on both the optical thickness and the value of the single scattering albedo for a given problem. However, we do not take on the matter of gaining the most efficiency from the one-way RTE here. Rather, we are focused solely on determining the accuracy of the one-way RTE in approximating the full RTE. To that end, we apply the method described in [24] to solve the initial value problem for the one-way RTE consisting of (3.13) with initial condition (3.15). A summary of this procedure is as follows.

1. Fourier transform (3.13) in x and y and make use of the axisymmetry inherent in this problem.
2. Solve the resulting problem using the discrete ordinate method described in several radiative transfer texts, e.g. [2,22,25,26].
3. Compute the diffuse transmittance given in (3.16) using a quasi-fast Hankel transform [27].

The procedure described above does not fully take advantage of the potential efficiency gains that the one-way RTE offers. Rather, we have chosen it because it allows us to solve both the full and one-way RTE using the same method. Consequently, we are able to compare the performance of the one-way RTE approximation without having to consider any additional issues introduced by using different methods. That being said, a key parameter to consider here is the order of the Gauss–Legendre

quadrature rule, M, used in the discrete ordinate method for the full RTE. Because the one-way RTE uses only the half-range of directions corresponding to the forward hemisphere, it only uses $M/2$ quadrature points, in comparison. Even though we have not explicitly sought to take advantage of the efficiency gains for the one-way RTE here, this reduction leads to an overall factor of 4 efficiency gain in solving the one-way RTE. For the various problems we study, we will have to vary M to ensure accurate results.

4. Numerical results

For all of the numerical results shown here, we have used 128 radial grid points to compute the quasi-fast Hankel transform. We assume that the refractive index on either side outside of the slab is the same, so any index-mismatch on both of the boundaries is solely determined by the relative refractive index, m, given by the ratio of the refractive index inside the slab over that outside the slab. In what follows, we evaluate comparisons of the full and one-way RTE as we vary (i) the anisotropy factor, g and the screening coefficient η, (ii) the single scattering albedo, ϖ_0, (iii) the optical thickness, z_0, and (iv) the relative refractive index, m.

4.1. Anisotropy factor

To study the one-way RTE as the anisotropy factor, g, varies, we study the diffuse transmittance with $\varpi_0 = 0.9$, $z_0 = 2$, $m = 1$, and beam radius $R = 0.5$. To ensure highly accurate results, we used a highly resolved angle grid with $M = 64$. Fig. 2 shows comparisons of the diffuse transmittance using the Henyey–Greenstein scattering phase function with $g = 0.7$, 0.8, and 0.9. The x-axis is the radial coordinate, $\rho = \sqrt{x^2 + y^2}$. For all the results shown in Fig. 2, we find that the qualitative agreement between one-way RTE and the full RTE is excellent. Indeed these results are all nearly indistinguishable from the full RTE results. In
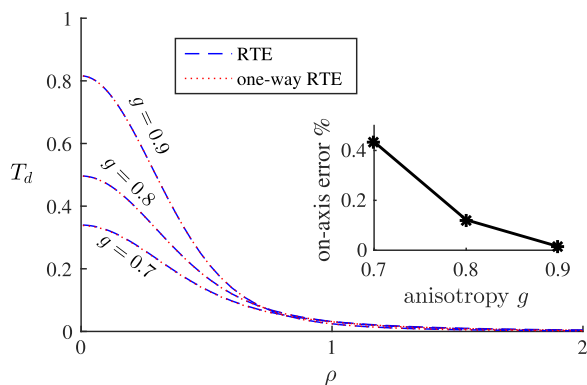

Fig. 2. Comparisons of the diffuse transmittance computed using simulations of the full RTE (solid curves) and the one-way RTE (dashed curves) as a function of the radial coordinate ρ for varying anisotropy factors: $g = 0.7$, 0.8, and 0.9. Here, $\varpi_0 = 0.9$, $z_0 = 2$, $R = 0.5$, and $m = 1$. The inset shows the on-axis ($\rho = 0$) relative errors made by the one-way RTE.
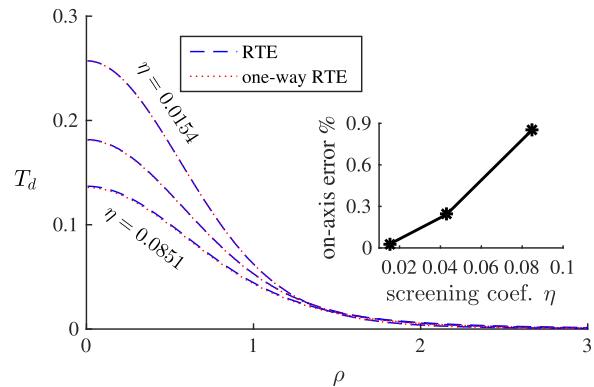

Fig. 3. Comparisons of the diffuse transmittance computed using simulations of the full RTE (solid curves) and the one-way RTE (dashed curves) as a function of the radial coordinate ρ for varying screening parameters: $\eta = 0.085$, 0.043, and 0.015. Here, $\varpi_0 = 0.9$, $z_0 = 2$, $R = 1$, and $m = 1$. The inset shows the on-axis relative errors made by the one-way RTE.

general, we find that the one-way RTE underestimates the diffuse transmittance, especially near its peak. To quantify this error, we have computed the on-axis error made by the one-way RTE defined as the absolute difference between the one-way RTE and the full RTE results divided by the full RTE result. Those on-axis error results are shown as an inset in Fig. 2. We see that on-axis relative error is less that 0.5% and decreases monotonically as g increases.

In Fig. 3, we show the diffuse transmittance using the screened Rutherford scattering phase function with screening parameters $\eta = 0.085$, 0.043, and 0.015. The beam radius is $R = 1$, but all other parameters are the same that were used for Fig. 2. These results are consistent with those shown in Fig. 2. These results for the one-way RTE with screened Rutherford scattering are also nearly indistinguishable from those of the RTE. The on-axis relative errors are all less that 1%. The inset of Fig. 3 shows that these on-axis relative errors grow monotonically with η.

4.2. Single scattering albedo

In deriving the one-way RTE, we have only assumed that scattering was forward peaked. We have made no assumption on the size of the single scattering albedo. Therefore, we anticipate that the one-way RTE should be valid across a broad range of single scattering albedo values. To verify this, we study the one-way RTE as the single scattering albedo, ϖ_0, varies.

Fig. 4 shows comparisons of the diffuse transmittance with Henyey–Greenstein scattering for $\varpi_0 = 0.5$, 0.7, and 0.9. The anisotropy factor is $g = 0.9$, the optical thickness is $z_0 = 2$, the relative refractive index is $m = 1$, and beam radius $R = 1$. We used a moderately resolved angle grid with $M = 32$ for these results since the demands on angular resolution are not too great for these problems.

Fig. 4 shows that the one-way RTE is accurate over this broad range of single scattering albedo values. The inset of Fig. 4 shows that the on-axis relative error is below 1% and monotonically decreases as ϖ_0 increases. This behavior is to be expected since stronger scattering increases the

importance of the forward-peak of the scattering phase function in the solution of the RTE.

4.3. Optical thickness

To study the one-way RTE as the optical thickness, z_0, varies, we compute the diffuse transmittance with $\varpi_0 = 0.9$, $g=0.9$, $R=1$, and $m=1$. Fig. 5 shows comparisons of the diffuse transmittance with Henyey–Greenstein scattering for $z_0 = 2$, 5, and 10. For these results, we used a slightly higher resolved angle grid with $M=40$ since a higher accurate solution is needed to accurately capture the behavior of the solution as z_0 increases.

In all of the results shown in Fig. 5, we find that the one-way RTE and full RTE simulations agree rather well. Indeed, the results are nearly indistinguishable from one another. The inset of Fig. 5 shows that the on-axis error increases monotonically as z_0 increases. However, the off-axis errors become substantially large even though that is not apparent in Fig. 5.

This degradation of accuracy of the one-way RTE approximation as z_0 increases can be understood as follows. As the beam penetrates more deeply in an optically thick medium, more power is continually exchanged between forward and backward directions. Eventually, this continual exchange of power flow saturates which, in turn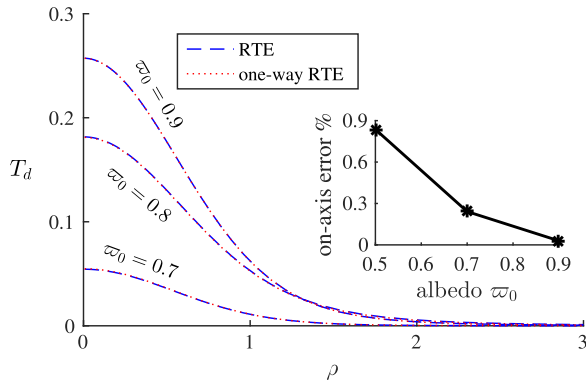, leads to the intensity becoming nearly isotropic. This saturation limit corresponds to the diffusion approximation, which applies when the scattering medium is optically thick [2]. Because it only governs the forward half-range intensity, the one-way RTE has no mechanism to take into account this exchange between forward and backward flowing powers. As a result, the one-way RTE is inherently unable to describe an isotropic intensity and, therefore, does not approach to the diffusion approximation for optically thick media. Nonetheless, we find that the one-way RTE is fairly accurate for small to moderate optical thicknesses.

We remark that the diffusion approximation reduces the RTE to a partial differential equation, which is significantly easier to solve. For this reason, the diffusion approximation has been used extensively, especially for biomedical optics. However, the diffusion approximation is only valid for optically thick media, and even then, it suffers from large errors near sources and boundaries. To address the errors made by the diffusion approximation near sources, Vitkin et al. [28] introduced the so-called phase function corrected diffusion approximation. By decomposing the scattering phase function into three terms: a delta function, an isotropic part, and an anisotropic part, Vitkin et al. derive an additive correction to the diffuse reflectance that improves the accuracy near the point-of-entry. Alternatively, one can correct the errors made by the diffusion approximation near sources and boundaries using boundary layer analysis [29]. However, this formal and systematic analysis necessarily adds some complexity back into the problem. Regardless, the diffusion approximation is limited only to optically thick media. In contrast, the one-way RTE approximation is valid for small to moderate optical thicknesses. In that way, it is complimentary to the diffusion approximation.

4.4. Refractive index

We study the one-way RTE as the relative refractive index, m, varies. In particular, we study the diffuse transmittance with $\varpi_0 = 0.9$, $g=0.9$, $z_0 = 2$, and $R=1$. We used a moderately resolved angle grid with $M=32$ for these results. Fig. 6 shows comparisons of the diffuse transmittance with Henyey–Greenstein scattering for $m=1.0$, 1.2, and 1.4.

Fig. 4. Same as Fig. 2, but for varying albedo, $\varpi_0 = 0.5$, 0.7, and 0.9. Here, $g=0.9$, $z_0 = 2$, $R=1$, and $m=1$.
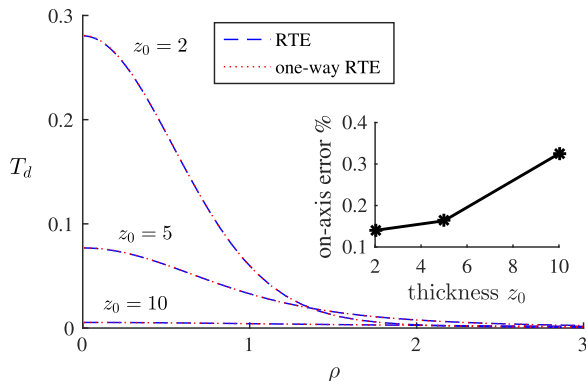

Fig. 5. Same as Fig. 2, but for varying thickness, (a) $z_0 = 2$, (b) $z_0 = 5$, and (c) $z_0 = 10$. Here $\varpi_0 = 0.9$, $g=0.9$, $R=1$, and $m=1$.
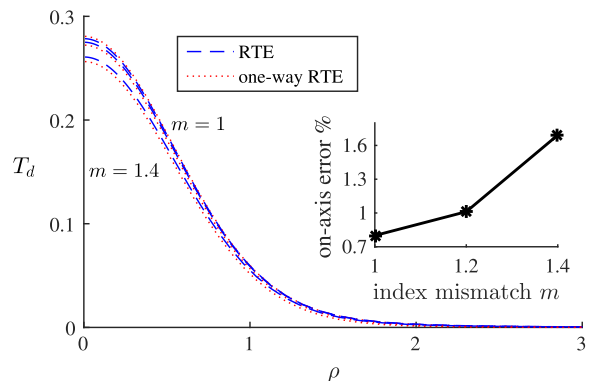

Fig. 6. Same as Fig. 2, but for varying refractive index mismatch, $m=1.0$, 1.2, and 1.4. Here, $\varpi_0 = 0.9$, $g=0.9$, and $z_0 = 2$.

In each of these results, we find that the one-way RTE qualitatively captures the RTE results. However, visible quantitative errors appear for $m > 1$. Since the partial reflection due to the index-mismatched boundaries provides another mechanism to exchange power from forward to backward flowing directions, one might assume that the one-way RTE will not be accurate for index-mismatched boundaries. In fact, the index-mismatched boundary at $z = z_0$, where light is transmitted, will redistribute a fraction of the forward flowing power backward. However, for this reflected light to eventually contribute to the diffuse transmittance, it must either backscatter thereby being redirected as forward flowing light, or be partially reflected by the boundary $z = 0$. Provided that the assumptions making the one-way RTE are valid, both of these effects are negligible. The results shown in Fig. 6 are consistent with this reasoning. The inset of Fig. 6 shows the on-axis errors to be less that 2% and that this error grows monotonically with m.

5. Conclusions and discussion

We have introduced the one-way RTE for modeling the transmission of a beam in a forward-peaked scattering medium. This approximation neglects the backscattered radiation. Unlike Fokker–Planck type approximations, the one-way RTE is not limited to sharply-peaked forward scattering. On the other hand, as an initial value problem, the one-way RTE is much easier to solve. The one-way RTE resembles the small-angle approximation, inasmuch as both are initial value problems. However, the one-way RTE retains a more accurate dependence between the angular and spatial nature of the radiation. The one-way RTE can also be interpreted as the first iteration in the improved source-iteration method for solving the full RTE. In this sense, the one-way RTE model is a physically meaningful manifestation of an improved numerical method.

Our numerical results show that the one-way RTE effectively approximates the diffuse transmittance of a Gaussian beam incident on a slab composed of a uniform absorbing and scattering medium. In particular, the one-way RTE accurately approximates the diffuse transmittance for (i) moderately large anisotropy factors, (ii) a broad range of single scattering albedo values, (iii) small-to-moderate optical thicknesses, and (iv) index-mismatched boundaries. The on-axis error monotonically decreases as the anisotropy factor and the single scattering albedo increase. It monotonically increases as the optical thickness and relative refractive index increase. Among these parameters, the error made by the one-way RTE is largest with respect to the relative refractive index.

These results are encouraging for using the one-way RTE to model the transmission of light in forward scattering media. One apparent limitation is that the one-way RTE is limited to studying transmission problems. For reflectance problems, one may consider extending the one-way RTE by using the results here to inform the computation of another one-way RTE for the backward half-range intensity. This extension is essentially Step 3 of the iteration method described in Section 3.2. Applying these ideas to the vector

radiative transfer equation that models multiple scattering of partially polarized light is also straight forward extension of what we have done here.

References

[1] Chandrasekhar S. Radiative transfer. New York: Dover Publications Inc.; 1960.
[2] Ishimaru A. Wave propagation and scattering in random media. New York: Wiley-IEEE-Press; 1999.
[3] Thomas G, Stamnes K. Radiative transfer in the atmosphere and ocean, atmospheric and space science. Cambridge: Cambridge University Press; 2002.
[4] Marshak A, Davis A. 3D radiative transfer in cloudy atmospheres, physics of Earth and space environments. Berlin: Springer; 2005.
[5] Wang L, Wu H. Biomedical optics: principles and imaging. Hoboken: Wiley; 2007.
[6] Pomraning GC. The Fokker–Planck operator as an asymptotic limit. Math Models Methods Appl Sci 1992;2(1):21–36.
[7] Larsen EW. The linear Boltzmann equation in optically thick systems with forward-peaked scattering. Prog Nucl Energy 1999;34(4): 413–23.
[8] Pomraning GC. Higher order Fokker–Planck operators. Nucl Sci Eng 1996;124(3):390–7.
[9] Prinja AK, Pomraning GC. A generalized Fokker–Planck model for transport of collimated beams. Nucl Sci Eng 2001;137(3):227–35.
[10] Leakeas CL, Larsen EW. Generalized Fokker–Planck approximations of particle transport with highly forward-peaked scattering. Prog Nucl Energy 2001;137(3):236–50.
[11] González-Rodríguez P, Kim AD. Light propagation in tissues with forward-peaked and large-angle scattering. Appl Opt 2008;47(14): 2599–609.
[12] Budak VP, Korkin SV. On the solution of a vectorial radiative transfer equation in an arbitrary three-dimensional turbid medium with anisotropic scattering. J Quant Spectrosc Radiat Transfer 2008;109 (2):220–34.
[13] Efremenko D, Doicu A, Loyola D, Trautmann T. Small-angle modification of the radiative transfer equation for a pseudo-spherical atmosphere. J Quant Spectrosc Radiat Transfer 2013;114:82–90.
[14] Rossi B, Greisen K. Cosmic-ray theory. Rev Mod Phys 1941;13: 240–309.
[15] Börgers C, Larsen EW. Asymptotic derivation of the fermi pencil-beam approximation. Nucl Sci Eng 1996;123(3):343–57.
[16] Börgers C, Larsen EW. On the accuracy of the Fokker–Planck and fermi pencil beam equations for charged particle transport. Med Phys 1996;23(10):1749–59.
[17] Su B, Pomraning G. The fermi beam solution generalized to oblique incidence. Ann Nucl Energy 1996;23(8):695–709.
[18] Claerbout JF. Toward a unified theory of reflector mapping. Geophysics 1971;36(3):467–81.
[19] Claerbout JF. Imaging the Earth's interior. Cambridge, MA, USA: Blackwell Scientific Publications, Inc.; 1985.
[20] González-Rodríguez P, Kim AD. Diffuse optical tomography using the one-way radiative transfer equation. Biomed Opt Express 2015;6 (6):2006–21.
[21] Borcea L, Garnier J. Derivation of a one-way radiative transfer equation in random media, Phys Rev E 93, 2016, 022115.
[22] Lewis EE, Miller WFJ. Computational methods of neutron transport. La Grange Park: American Nuclear Society; 1993.
[23] Gao H, Zhao H. A fast-forward solver of radiative transfer equation. Transp Theory Stat Phys 2009;38(3):149–92.
[24] Kim AD, Moscoso M. Beam propagation in sharply peaked forward scattering media. J Opt Soc Am A 2004;21(5):797–803.
[25] Modest M. Radiative heat transfer, chemical, petrochemical & process. Boston: Academic Press; 2003.
[26] Howell J, Menguc M, Siegel R. Thermal radiation heat transfer. 5th edition, Boca Raton: CRC Press.; 2011.
[27] Siegman A. Quasi fast Hankel transform. Opt Lett 1977;1(1):13–5.
[28] Vitkin E, Turzhitsky V, Qiu L, Guo L, Itzkan I, Hanlon EB, et al. Photon diffusion near the point-of-entry in anisotropically scattering turbid media. Nat Commun 2011;2:587.
[29] Kim AD. Correcting the diffusion approximation at the boundary. J Opt Soc Am A 2011;28(6):1007–15.